Supplementary Material

Incorporating silicon carbide nanoparticles into Al_2O_3@Al as efficient support for Co-based catalyst to boost the catalytic performance toward Fischer-Tropsch Synthesis

Min Zhong [a,b], Jungang Wang [a], Congbiao Chen [a], Zhancheng Ma [a] , Litao Jia [a,c], Bo Hou [a*] and Debao Li [a,c*]

[a] *State Key Laboratory of Coal Conversion, Institute of Coal Chemistry, Chinese Academy of Sciences, Taiyuan 030001, Shanxi, PR China*

[b] *University of Chinese Academy of Sciences, Beijing 100049, PR China*

[c] *Dalian National Laboratory for Clean Energy, Dalian, 116023, China*

Corresponding author: Bo Hou (houbo@sxicc.ac.cn), Debao Li (dbli@sxicc.ac.cn);

Fax: (+86) 0351-4041153. Tel: (+86) 0351-4121877

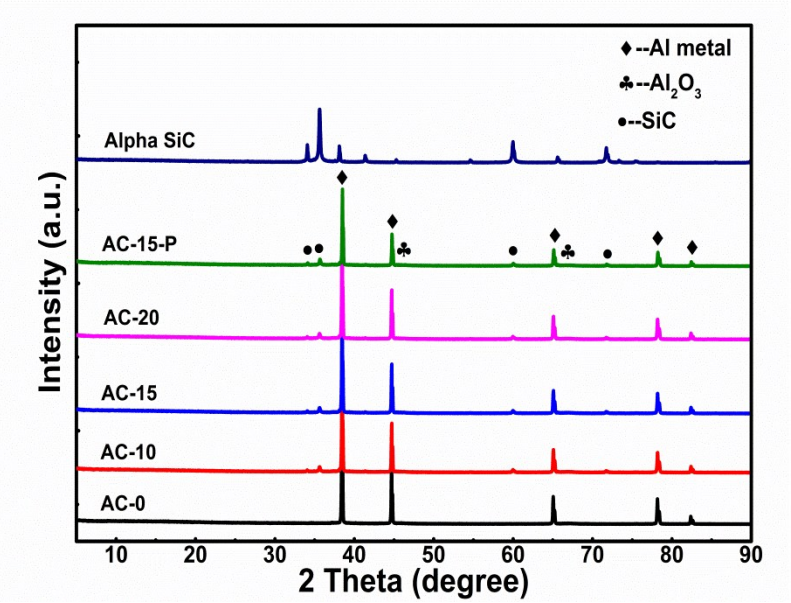

Fig. S1 XRD patterns of supports

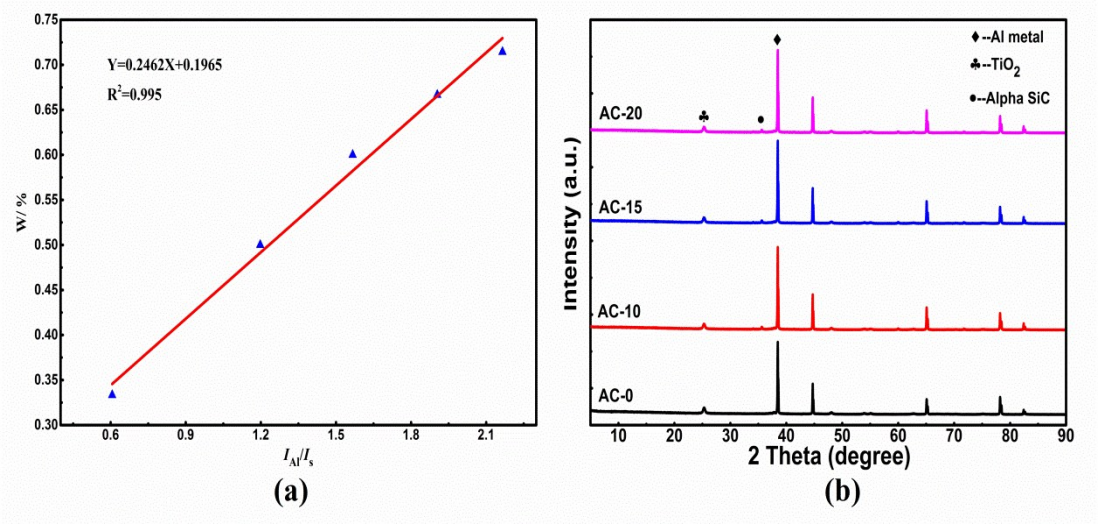

Fig. S2 quantitative X-ray diffraction (XRD) method to estimate the metallic Al content: a) working curves for quantitative analysis of metallic Al; b) XRD patterns of support samples

A quantitative X-ray diffraction (XRD) method with anatase TiO_2 as an internal standard was used to estimate the content of metallic Al for the supports. The XRD patterns of the mixture of Al metal powders and TiO_2 with different mass ratios were used to model the working curve for quantitative analysis of metallic Al. The I_{Al}/I_s as the abscissa (X) and w% (Y, the content of metallic Al) as the ordinate, the working curves (Y= 0.2462X+0.1965) was obtained by fitting the test data (Fig. S2a). The XRD pattern of support samples with 20% internal standard TiO_2 to get the I_{Al}/I_s value (Fig. S2b), and then calculated the content of metallic Al for AC-x supports.

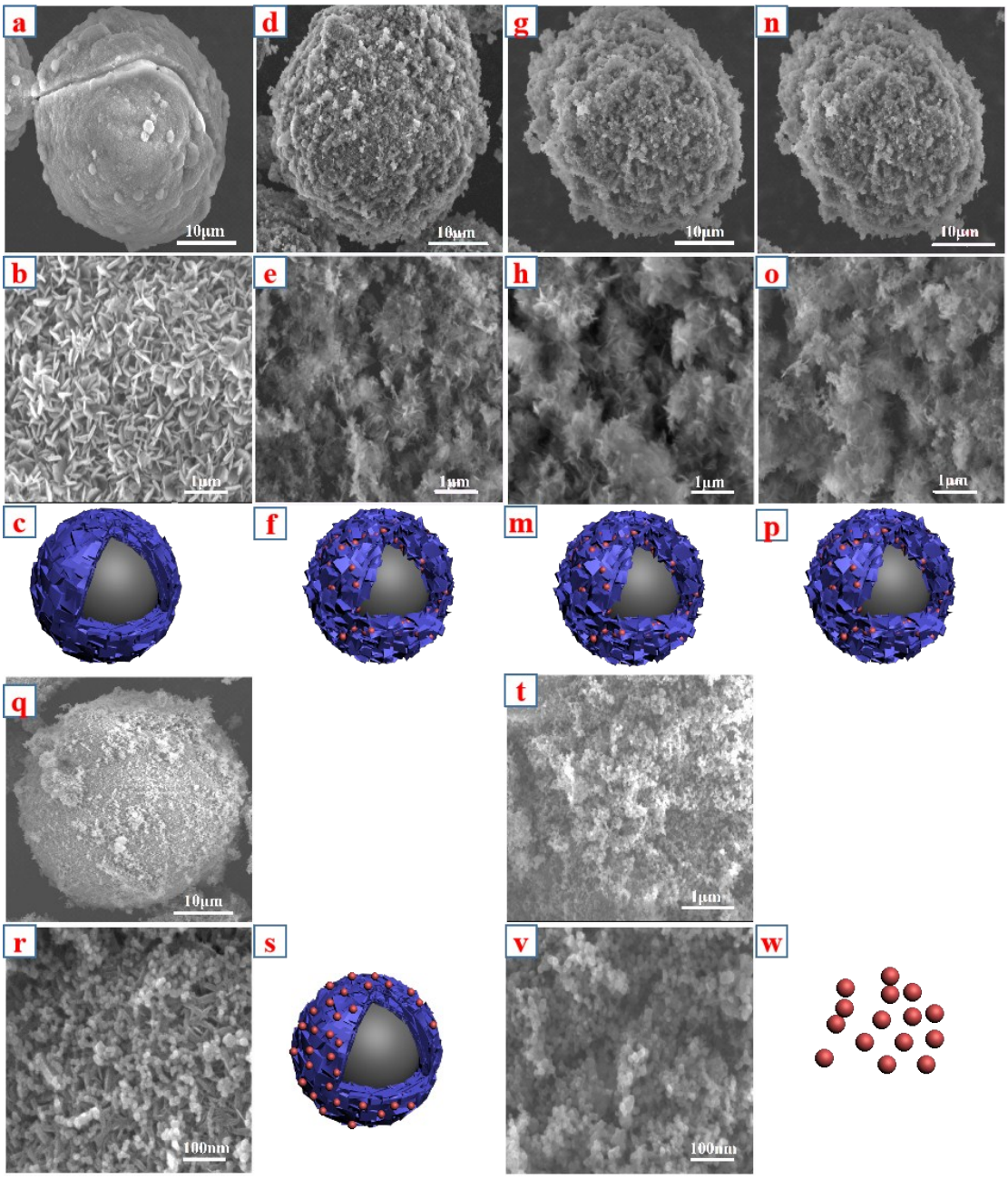

Fig. S3 The SEM images and model of supports: a, b, c) AC-0; d, e, f) AC-10; g, h, m) AC-15; n, o , p) AC-20; q, r, s) AC-15-P; t, v, w) SiC NPs

The Fig. S3 displayed the microtopography of the AC-x/ AC-15-P composites and alpha SiC NPs determined by SEM measurements, and the schematic diagram which the distribution of SiC NPs in AC-x and AC-15-P composites. As could be seen, large amount of SiC NPs were located on on the surface of AC-15-P sample. However, no obvious SiC NPs or clusters were observed on the surface of AC-10, 15, 20 composites, suggesting that SiC NPs and AlOOH formed binary structure during hydrothermal synthesis rather than existed alone.

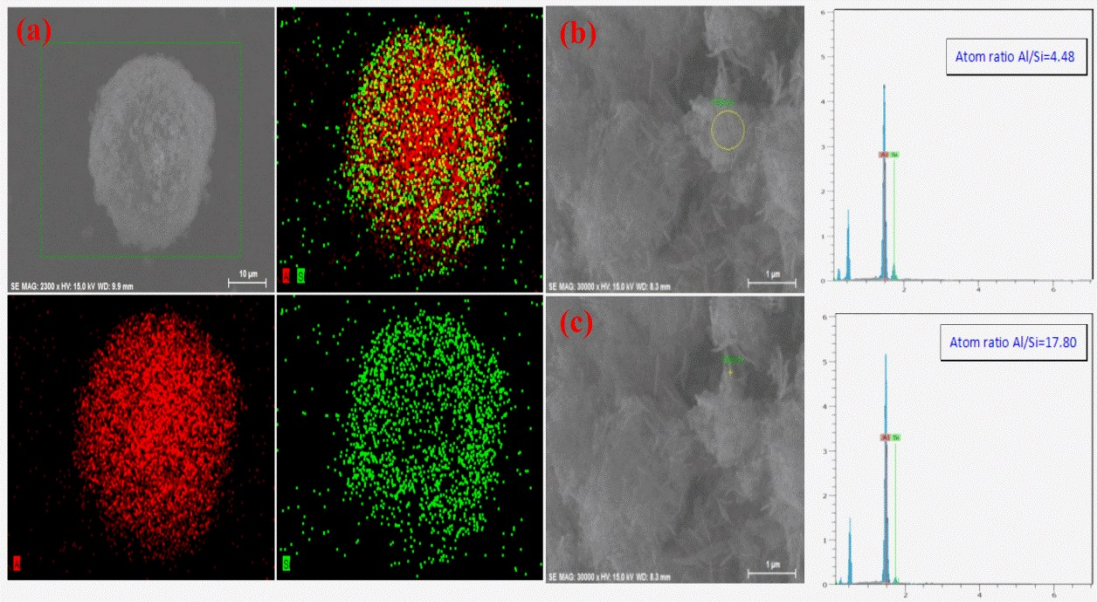

Fig. S4 SEM analysis of AC-15 support: a) elemental mapping; b) the atom ratio of Al to Si for "slice-like" structure; b) the atom ratio of Al to Si for small rough particles

The shell of AC-15 composite was composed of irregular "slice-like" structure and roughly spherical particles, we used the EDS to confirm the composition of the two parts, as shown in Fig. S4. The Al/Si atom ratio was 17.80 for irregular "slice-like" structure (Fig. S4c), suggesting that this structure was mainly made up with Al_2O_3. While Al/Si atom ratio was 4.48 for roughly spherical particles, meaning that this structure was composed of SiC and Al_2O_3 (Fig. S4b). The elemental mapping of individual particle of AC-15 composite showed that the Si and Al elements were dispersed well on composite surface (Fig. S4a).

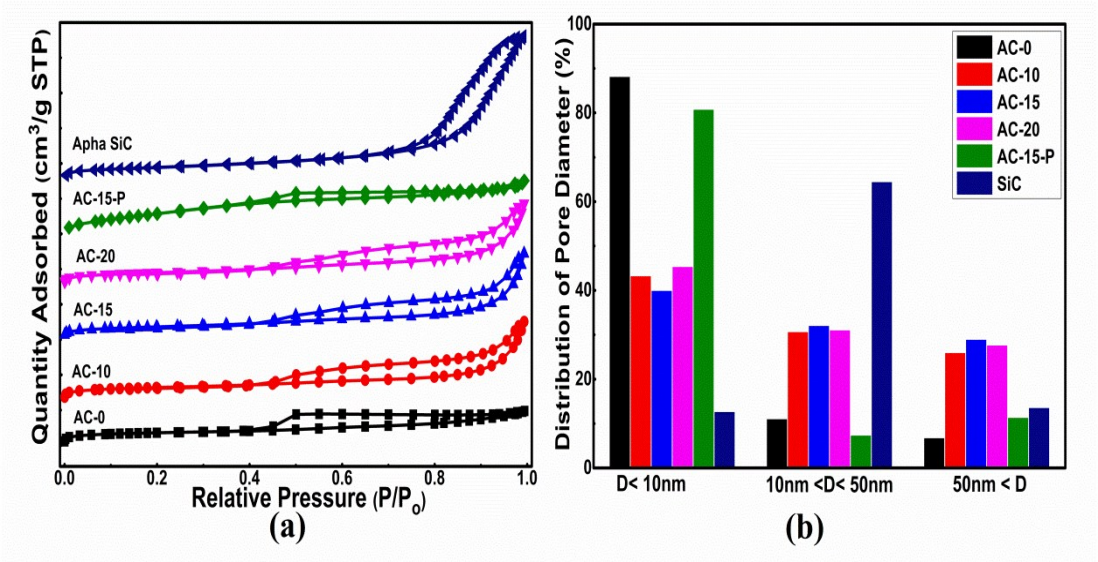

Fig. S5 The N_2-physirption of the supports: a) N_2-adsorption/desorption isotherms; b) the pore size distribution

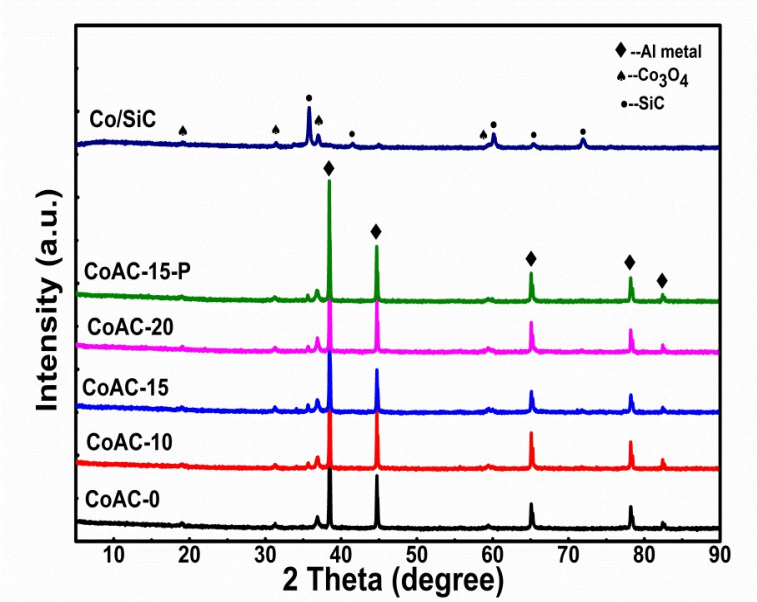

Fig. S6 XRD patterns of catalysts

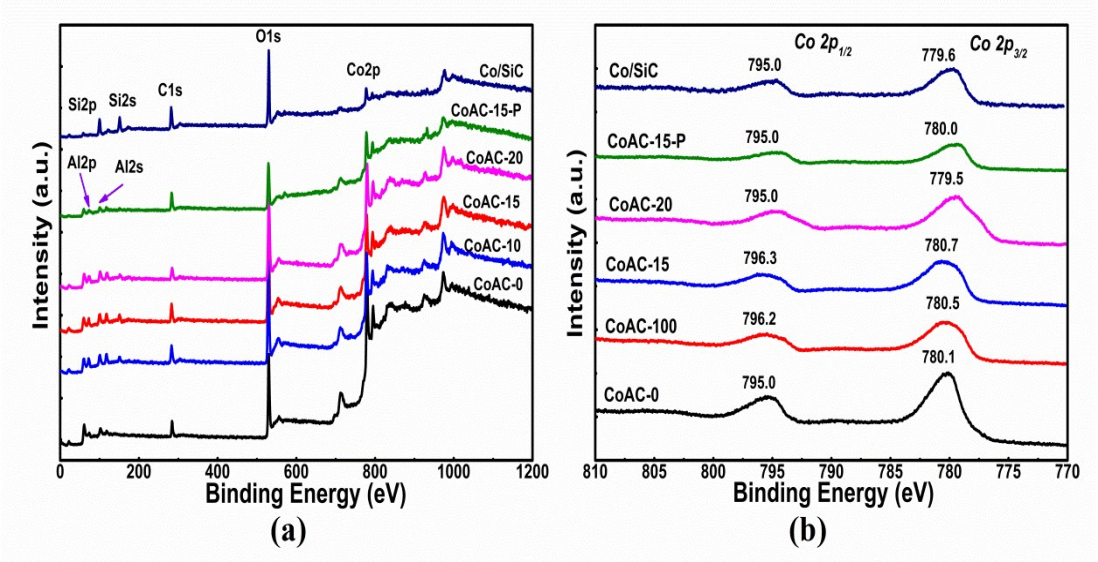

Fig. S7 XPS spectra of catalysts: a) wide spectra; b) Co 2p

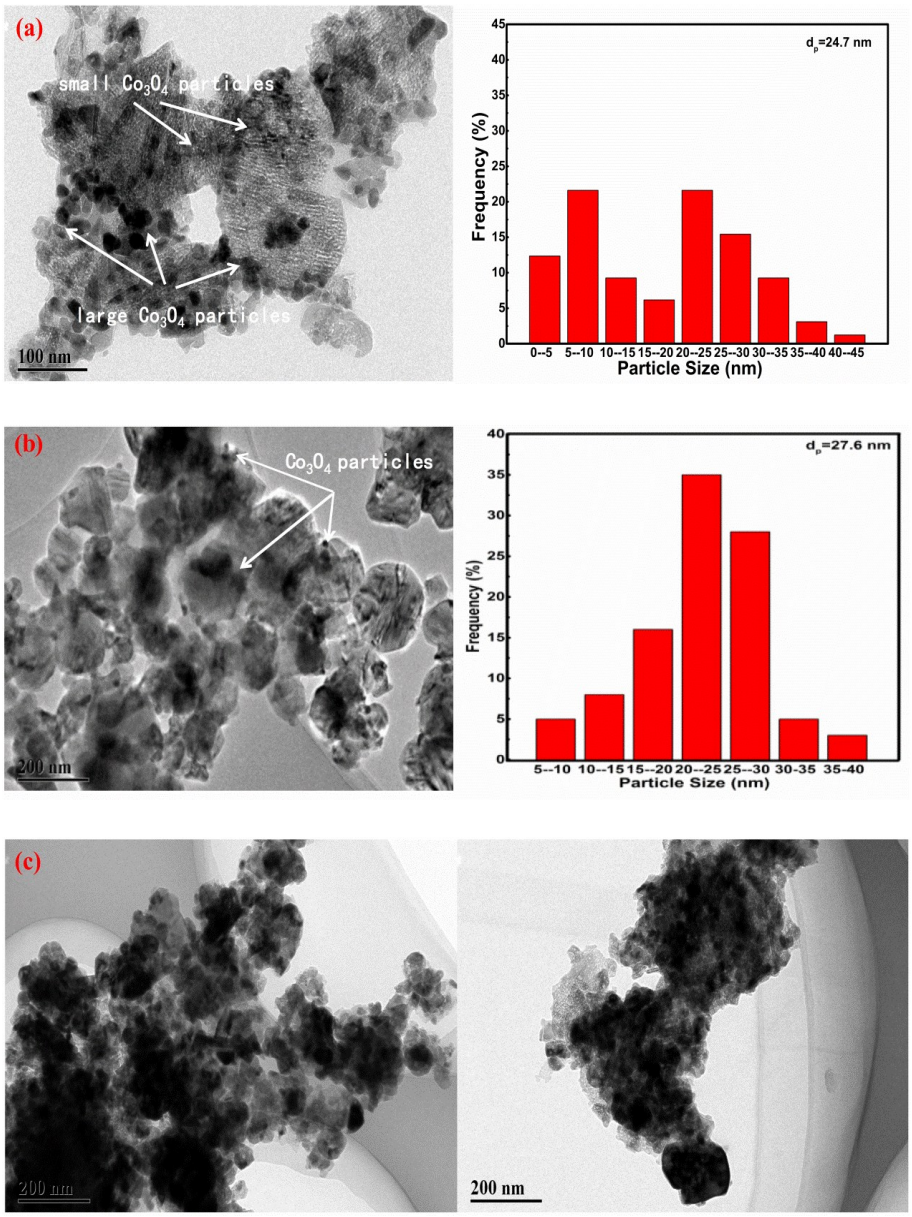

Figure S8 TEM images and corresponding Co particle size distribution of catalyst samples: a) CoAC-0; b) Co/SiC; c) CoAC-15

Fig. S8 was the TEM images of the catalysts. Due to strong cobalt-support interaction, the $Co/Al_2O_3@Al$ catalyst had a considerable fraction of small cobalt particles. However, the inert surface chemistry of SiC led to weak cobalt-support interaction, as a result, the cobalt particles in Co/SiC sample were mainly large one. Because the morphology and size of cobalt oxide particles were similar to SiC NPs, it was impossible to distinguish cobalt NPs from SiC NPs in CoAC-15 sample. Nevertheless, the number of small NPs in CoAC-15 catalyst was very small. Therefore, the interaction between Co and supports could still be indirectly distinguished by the particle size distribution of cobalt.

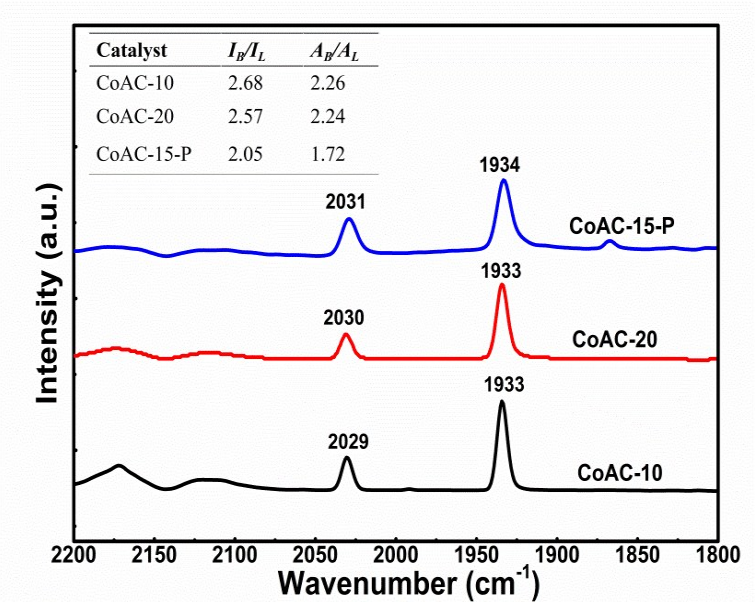

Fig. S9 In situ DRIFT spectra of CO adsorption on the reduced catalysts. *I*, intensity of absorption; *B*, bridged absorption; *L*, linear absorption; *A*, area of integrated absorption

Table S1 The content of composition in the catalysts determined by the ICP measurements

Catalyst	**Co (%)** [a]	**SiC (%)**	**Al_2O_3 (%)** [b]
CoAC-0	14.1	0	24.5
CoAC-10	14.5	6.2	14.2
CoAC-15	14.6	10.8	11.6
CoAC-20	14.2	14.5	9.4
CoAC-15-P	14.2	11.5	15.5
Co/SiC	15.6	70.4	0

[a] Assuming that Co elements existed in the catalyst in the form of Co_3O_4; [b] Al elements existed in the catalyst in the form of Al_2O_3 and Al metal.

The ICP analysis was used to measure the content of SiC, Al_2O_3, Al metal and Co in catalyst samples, and the data was listed in Table S1. Assuming that SiC NPs were insoluble, Co and Al elements existed in the catalyst in the form of Co_3O_4, Al_2O_3 and Al metal respectively.